

Invertibility of a 1-D Discrete Ordinates Canopy Reflectance Model

J. L. Privette,^{*,†} R. B. Myneni,^{‡,§} C. J. Tucker,[‡] and W. J. Emery^{*}

The invertibility of an accurate discrete ordinates canopy reflectance model is investigated through a series of experiments. Effects of different canopy types, noise levels, spectral ranges, and sampling geometries [including the NOAA Advanced Very High Resolution Radiometer (AVHRR) and the proposed Multi-angle Imaging SpectroRadiometer (MISR) satellite sampling schemes] are considered. Both error-free synthetic bidirectional reflectance data and empirical field reflectance data are utilized. Results suggest that the model can retrieve soil and canopy parameters with reasonable accuracy in most cases, and surface state parameters (absorbed radiation, spectral albedo and photosynthetic efficiency) with high accuracy in all cases. The efficiency of several commonly used optimization algorithms is also assessed, and a model sensitivity study is conducted.

INTRODUCTION

A large number of analytical and numerical models of surface bidirectional reflectance distribution functions (BRDFs) have been developed in recent years for applications in optical remote sensing (Myneni and Ross, 1991). These models have been validated with empirical data to varying degrees of accuracy and inverted to estimate surface variables. A successful inversion generally allows the retrieval of several independent model

parameters which may have biological or climatological significance. An inversion may further allow the calculation of surface state variables [e.g., spectral albedo, absorbed photosynthetically active radiation (APAR), canopy photosynthetic efficiency (CPE), etc.] from a limited set of empirical reflectance values depending on the stability and uniqueness of the problem. Thus, model inversions with satellite remote sensing data could potentially provide important land surface information for use in global climate, biogeochemical, ecological, and plant growth models (Dickinson, 1983; Wessman et al., 1991; Prince, 1991).

Goel and his colleagues pioneered the study of vegetation BRDF inversions as detailed in a series of papers beginning in 1983. After developing an appropriate problem definition, merit function and inversion strategy (Goel and Strebel, 1983), they inverted several 1-D BRDF models—most notably the Suits (1972), SAIL (Verhoef, 1984), and Cupid (Norman, 1979) models—and quantified parameter relationships and model sensitivity. Using a different modeling approach, Strahler and his colleagues developed and inverted a reflectance model which simulates a heterogeneous vegetation canopy as an assortment of geometrical objects. Estimates of tree crown size and density were retrieved (Li and Strahler, 1985). Antyufeev and Marshak (1990) developed a turbid medium BRDF model and successfully inverted it using Monte Carlo techniques. They retrieved three optical and four geometrical canopy parameters from reflectance data at two wavelengths. The hybrid 3-D model developed by Norman and Welles (1983) combines the geometrical objects and turbid medium approaches to simulate the BRDFs of heterogeneous vegetation canopies. This model has been inverted by Goel somewhat less successfully (Goel, 1992, personal communication). Recently, simple analytical models have been developed and inverted specifically for application to climate models (Pinty et al., 1990; Dickinson et al., 1990). These models lack some of the

^{*} Department of Aerospace Engineering Sciences, University of Colorado, Boulder

[†] DOE Global Change Graduate Fellow

[‡] Biospheric Sciences Branch, NASA/Goddard Space Flight Center, Greenbelt

[§] Universities Space Research Association Resident Associate

Address correspondence to Jeffrey L. Privette, CB 431, Dept. of Aerospace Engineering Sci., Univ. of Colorado, Boulder, CO 80309-0431.

Received 28 March 1993; revised 24 July 1993.

physical rigor found in other models but are designed for computational efficiency. Finally, Kuusk (1994) combined the single scattering formulation of the Nilson–Kuusk model (1989) with the diffuse scattering formulation of the SAIL model to produce a computationally-efficient invertible model. The new model has been validated against results from SAIL, the Nilson–Kuusk model, and a radiosity model (Goel and Kuusk, 1992). A valuable review of inversion studies for vegetation remote sensing is contained in a recent monograph (Goel, 1988).

In this initial study, the invertibility of a model based on an accurate numerical solution of the 1-D vegetation radiative transfer equation (Shultis and Myneni, 1988) is investigated. The accuracy of the retrieved model parameters [leaf area index (LAI), leaf normal distribution function, leaf and soil optical properties, and a hot spot parameter] and the surface state variables [fraction of APAP (FAPAR), CPE, spectral albedo, and fraction of absorbed near-infrared radiation (FANIR)] is assessed at several points in the problem domain to ascertain the practical limitations of numerical model inversions.

The outline of this article is as follows: First, model details are discussed to the extent necessary for later discussion. A general inversion procedure is presented next, followed by an assessment of different minimization routines. Several standard problems are then proposed to construct synthetic BRDF data sets. The model is inverted with these data sets, and the results are discussed. These inversions utilize BRDFs sampled in the complete upper hemisphere. Inversions using satellite system sampling geometries are also presented. The effects of random noise in the BRDF data are evaluated with respect to the accuracy of retrieved variables. Finally, the inversion of empirical BRDF data is presented, followed by conclusions and general remarks.

MODEL DESCRIPTION

CANTEQ is a 1-D turbid medium BRDF model based on the discrete ordinates solution to the radiative transfer equation (Shultis and Myneni, 1988; Stewart, 1990). The turbid medium concept, initially suggested by Shifrin (1953) and generalized by Ross (1981) for vegetation canopies, models a homogeneous surface as a cloud of infinitesimal platelets of statistically prescribed orientation. Although mathematically attractive, one disadvantage of the turbid medium concept is the absence of scattering characteristics due to the size of the scatterers (e.g., the hot spot). Therefore, following Marshak (1989), a canopy hot spot approximation is included in CANTEQ by adjusting the canopy extinction coefficient for the once-scattered radiation (Stewart, 1990).

The statistical orientation of platelets in the turbid medium mimics the leaf angle distribution (LAD) of a canopy. While the initial model configuration permitted

five idealized LADs (planophile, erectophile, plagio-ophile, extremophile, and uniform), a more recent extension utilizes the continuous Beta LAD (Goel and Strebel, 1984). Anisotropic leaf scattering is included using the bi-Lambertian diffuse leaf reflectance and transmittance model proposed by Ross and Nilson (Ross, 1981). In addition, a specular leaf reflection formulation (Vanderbilt and Grant, 1985; Nilson and Kuusk, 1989) is coupled to the bi-Lambertian model to simulate the leaf scattering phase function.

A Lambertian soil represents the bottom boundary layer. Since soil BRDFs are in general anisotropic (Eaton and Dirmhirn, 1979), the absence of soil anisotropy in the model decreases its validity at low LAI. The upper boundary condition includes direct solar irradiance plus isotropic diffuse irradiance.

The discrete ordinates method is used to solve the radiative transport equation. In this method, photons are restricted to travel in a finite number of directions. These directions are chosen to be the ordinates of a quadrature scheme such that the angular integrals are evaluated accurately. The spatial derivative is approximated by a finite difference scheme, resulting in a system of algebraic equations that can be solved by iteration on the scattering integral. Methods to accelerate this iteration are also included in CANTEQ. All calculations in this study utilized six ordinates per octant for a total of 48 directions in the unit sphere. The model has been validated against reflectance data from soybean (Myneni et al., 1988), maize (Myneni et al., 1988), prairie grassland (Asrar et al., 1989) and several other agricultural crops (Stewart, 1990).

Photosynthetic efficiency values are calculated via a semiempirical leaf physiology model (Collatz et al., 1991) coupled to the BRDF model. The physiology model was developed for C_3 species and gives net photosynthesis as a function of environmental and leaf parameters and stomatal conductance. In this study, model parameters were assigned values representative of those generally encountered in practice.

INVERSION PROCEDURES

The general inversion problem may be stated as follows: Given a set of empirical directional reflectance measurements, determine the set of independent model parameters such that the computed directional reflectances best fit the empirical directional reflectances. The fit of the empirical data is determined by the merit function (Goel and Strebel, 1983), ϵ^2 , defined here as

$$\epsilon^2 = \sum_{j=1}^n [r_j - r_{jm}]^2 \quad (1)$$

where r_j is the directional reflectance for a given scan and solar angle geometry, r_{jm} is the geometrically-analogous model estimate, and n is the number of reflectance samples.

Initially, five independent parameters were adjusted to minimize the value of the merit function: LAI, a hot spot parameter (related to the ratio of canopy height to characteristic leaf dimension), leaf hemispherical reflectance and transmittance, and soil hemispherical reflectance. The Beta distribution model for the leaf normal orientation added two more parameters (μ and ν) to this set. While additional independent parameters generally allow a better fit of the empirical data, the statistical significance of the retrieved parameter estimates decreases (Goel and Thompson, 1984c).

A penalty function is required to limit the independent parameter space to physically possible values. Moreover, the sum of leaf reflectance and transmittance (the leaf albedo, ω) can be constrained, based on physical arguments, such that $0 < \omega < 1.0$. Therefore, the following modification to the merit function was employed:

$$\epsilon_p^2 = \sum_{j=1}^n [r_j - r_{jm}]^2 + \sum_{k=1}^p [(x_k - x_{kb})^2 w_k]^2, \quad (2)$$

where x_k is the value of parameter k , x_{kb} is the limiting value of parameter k , p is the number of constraints, and w_k is the penalty weight. For this study, $w_k = 0$ for $x_{kb,\min} < x_k < x_{kb,\max}$, and $w_k = 10^{20}$ otherwise. Such a penalty function greatly increases the merit function value when the parameters assume values outside the imposed limits. Once the best fit is achieved (ϵ_p^2 is minimized), the model parameters producing that fit are considered the retrieved parameters and the best estimates of the true surface values.

MINIMIZATION ALGORITHMS

Three commonly used minimization routines were tested in this study: a downhill simplex method (subroutine AMOEBA from Press et al., 1986), a conjugate direction set method (subroutine POWELL from Press et al., 1986), and a quasi-Newton method (subroutine E04JAF from Numerical Algorithms Group, 1990). These routines were chosen in part because they do not require function derivatives for minimization. This aspect is particularly appealing for complex, nonlinear formulations such as CANTEQ.

While complete algorithm description is beyond the scope of this article, differences between the three deserve some attention. The simplex method requires initial specification of the $P+1$ simplex vertices in the P -parameter space. Beginning with the vertex producing the largest merit function value (poorest fit), the algorithm systematically moves the vertex in an attempt to find a lower function value. This is repetitively continued. When all $P+1$ vertices produce fits to within a user-defined tolerance, "doneness" is achieved. While this routine is generally slower than others, it is considered robust and very useful for discontinuous functions

or functions subject to inaccuracies (Numerical Algorithms Group, 1990).

Beginning from a single initial position, the conjugate direction set method essentially conducts single line minimizations, accurate to within a user-defined tolerance, in each of the current P conjugate directions to arrive at the minimum for a given iteration. It then compares the current minimum to the previous iteration's minimum, and if the two estimates are within a second user-defined tolerance of each other, doneness is achieved. If the difference is greater than the allowed tolerance, the conjugate directions are redefined based on the vector between the two minima, and another iteration is executed.

The NAG quasi-Newton algorithm is similar to the direction set method in that it accumulates function information based on successive line minimizations. The two differ in the way they gather and store this gradient information. Unlike the direction set method, the quasi-Newton algorithm approximates the second partial derivative (Hessian) matrix at each iteration based on information for the latest search direction. It is efficient but intended for continuous functions with continuous first and second partial derivatives (Numerical Algorithms Group, 1990). In contrast to the direction set and simplex algorithms, the NAG quasi-Newton implementation does not require or allow a user-defined termination criteria.

In this study, the ability to specify termination criteria proved to be important. Figure 1 illustrates typical performances (change in merit function value ϵ^2 with number of function evaluations) of the three routines. The NAG routine consistently gave the poorest performance. In several inversions using synthetic reflectance data, the NAG routine indicated a best fit when the solution was incorrect (local trapping). This may be the result of having to use predefined rather than user-specified termination criteria. Furthermore, in cases where the NAG solution was correct, several thousand function evaluations were often required. The direction set method, in allowing user-specified tolerances, permitted tuning such that the routine could usually avoid local minima and find the correct solution. However, this tuning often resulted in an excessive number of function evaluations. The simplex algorithm, in contrast, consistently produced the best results. In cases where the quasi-Newton method produced incorrect solutions and where the direction set method produced the correct solution but required several thousand function evaluations, the simplex method efficiently found the correct solution in 500–600 function evaluations. The superiority of the simplex algorithm with respect to the others suggests the merit function may not have continuous first and second partial derivative throughout the parameter space. Based on these findings, the simplex algorithm was used exclusively for all subsequent inversions.

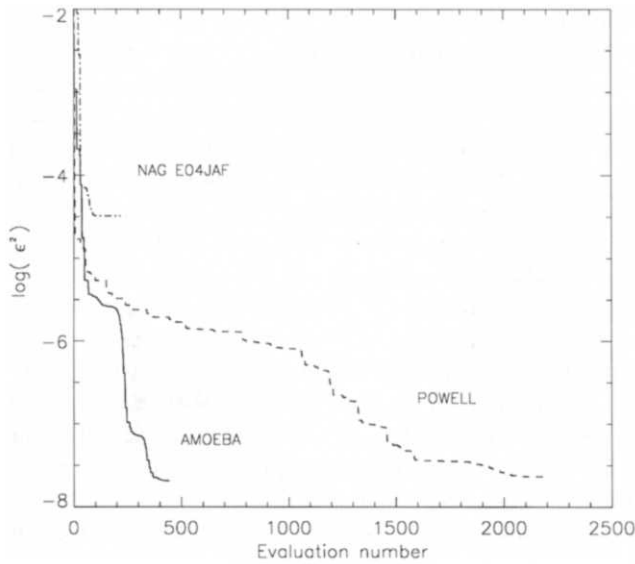
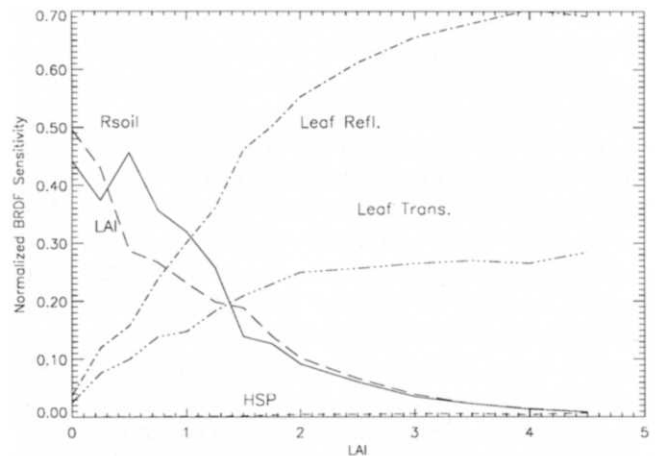


Figure 1. Convergence efficiencies, as shown by the log of the merit function, for optimally-tuned minimization routines AMOEBA, POWELL, and NAG E04JAF. The correct solution position was (LAI = 3.0, HSP = 4.0, leaf refl. = 0.0607, leaf trans. = 0.0429, soil refl. = 0.2). The inversion solution positions were AMOEBA (3.0, 4.1, 0.0608, 0.0426, 0.19), POWELL (3.0, 4.0, 0.0607, 0.0430, 0.20), and E04JAF (0.1, 2.0, 0.0001, 0.0001, 0.03). The initial positions for POWELL and E04JAF were the same.

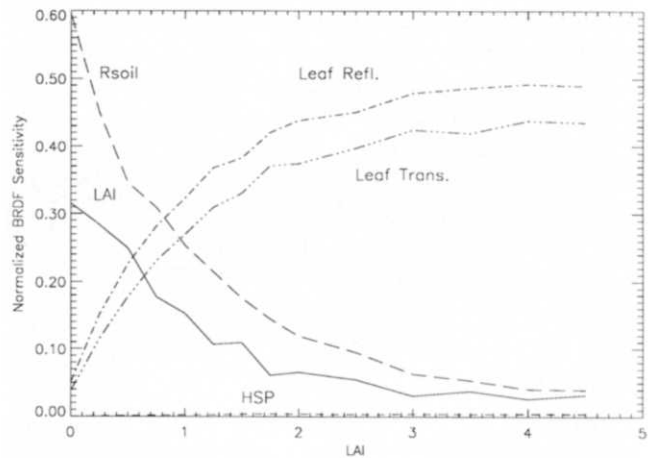
MODEL SENSITIVITY

Model sensitivity to each of the input parameters was tested initially. This required forward computation of a large number of synthetic BRDF sets. Bias was eliminated by using a random number generator to produce parameter values within reasonable and physically plausible limits. For a given synthetic canopy, each parameter was in turn perturbed by 10% of its theoretical range, and a new BRDF was computed. The sum of squares of differences between the original BRDF and the BRDF produced by a parameter's perturbation was recorded. This statistic was regarded as a measure of the model's sensitivity to that parameter. This exercise was conducted for 400 synthetic canopies at two different solar zenith angles. Principal component analysis was then performed on the sum of squares of differences. Since the first principal component axis, by definition, was in the direction of maximum variance, the numerical weighting of each parameter's contribution to that axis provided a measure of the model's relative sensitivity to the parameters.

The results of this analysis are shown for red and near-infrared wavelengths (NIR) in Figures 2a and 2b. While the two graphs are qualitatively similar, a closer inspection reveals some important differences. As might be expected, soil reflectance is most important in thin canopies (low values of LAI). At red, LAI is nearly



(a)



(b)

Figure 2. Normalized model sensitivity to five model parameters for increasing LAI at red (a) and NIR (b) wavelengths.

equally as important as soil reflectance in determining the canopy BRDF. At NIR, however, it is distantly second to soil reflectance. The highly absorbing leaves at red wavelengths can significantly decrease soil illumination and soil-reflected exiting radiance, whereas at NIR the highly scattering leaves have considerably less impact on the soil contribution. In both cases, the leaf optical properties have relatively minor influence in thin canopies. With an increase in LAI, however, model sensitivity to leaf optical properties increases at both wavelengths with a corresponding decrease in sensitivity to soil reflectance and LAI. The response lines cross at about LAI = 1.0 for both wavelengths. This suggests that, for canopies of LAI < 1.0, soil reflectance and LAI are most influential in determining the BRDF, whereas, for LAI > 1.0, leaf optical properties (reflectance and transmittance) are most influential. Beyond an LAI of about 2.0, the model is essentially insensitive to small changes in either LAI or soil reflectance. These sensitivi-

ties are consistent with those found by Goel et al. (1984) using SAIL and a more theoretical sensitivity analysis.

The NIR and red results differ significantly for optically thick canopies as well. In the red case, the model is considerably more sensitive to leaf reflectance than transmittance. Since the red leaf albedo is low, it is highly probable that the photons will be absorbed in one of the upper leaf layers. Even if a photon penetrates to the lower layers or to the soil, it is highly likely that the photon will be absorbed on its upwelling travel. Therefore, the influence of small changes in an already small value of leaf transmittance is minimized by high leaf absorption. In other words, the multiply scattered component of red radiance is insignificant compared to the once-scattered component. This fact explains the hot spot peak in red reflectance. In the NIR, the model is nearly equally sensitive to small changes in both the leaf reflectance and transmittance. The contribution of multiple scattering is significant at this wavelength. Thus, if a NIR photon penetrates the top canopy layers and is reflected by a lower layer or the soil, there is a high probability it will exit the canopy along the upwelling direction. Since both the leaf reflectance and transmittance determine this probability, both parameters significantly influence the net BRDF. The asymptotic tendency of the lines suggests that model sensitivity remains approximately the same for canopies of $LAI > 3.0$. It appears that the model is rather insensitive to small changes in the hot spot parameter at all optical depths.

This sensitivity analysis suggests which canopy parameters may be most accurately retrieved at a given LAI. Specifically, in multidimensional minimization procedures based on function values, the retrieved parameter values are not independent of each other. A substantial error in one retrieved parameter value will inevitably lead to errors in other parameters. Results suggest that the inversion process is best able to correctly retrieve those parameters to which the model is most sensitive. In effect, these most influential parameters are nearly independent of the less influential parameters for retrieval purposes. The more influential parameters remain, of course, somewhat dependent upon each other's retrieval accuracy.

INVERSION OF THE BASE CASE AND ITS PERTURBATIONS

Initial investigations of model invertibility were performed using synthetic BRDF sets created through forward model calculations. Directional reflectances at 15° zenith angle ($0-75^\circ$) and 45° azimuth angle ($0-180^\circ$) intervals were calculated. Since the model is symmetric about the principal plane, the reflectance distribution in the third and fourth octants provides no new information. In addition, radiation absorption, spectral albedo and CPE (at red) were evaluated (Myneni et al., 1992).

A standard atmosphere was assumed such that 80% of the incident irradiance was direct radiative flux.

A base case canopy was defined by assigning parameters values representative of those generally encountered in practice. A solar zenith angle of 30° and a uniform LAD were assumed. Perturbations to the base case were created by assigning widely varying but reasonable parameter values, one at a time. Tables 1a and 1b show the parameter values in the base and perturbed cases at red and NIR wavelengths. Note that leaf optical properties were perturbed only at the red wavelength. Since the LAD was not variable in these inversions, the planophile (erectophile) case denotes that, although the reflectance distribution was calculated with a uniform LAD, the inversion was attempted assuming a planophile (erectophile) LAD.

It should be noted that a perfect fit was not possible since the synthetic BRDF values were truncated at the fourth decimal place. The truncation was employed for two reasons: a) The computational results are unstable past four decimal places over different machines, and b) current field reflectance measurements are not accurate past four decimal places. Therefore, some minor discrepancies are to be expected in the retrieved parameters.

Results from the various inversions are shown in Figures 3a-d (red) though 4a-c (NIR). In general, most parameter values were retrieved to within about 5% of their true values. Inversions at the red wavelength produced significantly larger errors in five cases. In Case 7, denoting a dense canopy ($LAI = 8.0$), the inversion overestimated LAI by 23% and underestimated soil reflectance by 23%. This is not surprising since this canopy is optically semiinfinite and the model was found to be relatively insensitive to LAI for large LAI (Fig. 2a). Indeed, this insensitivity has been observed in empirical data for all spectral bands at sufficiently high LAI (Chance and LeMaster, 1977). In Case 10, denoting dark leaves (leaf optical properties halved), the inversion underestimated leaf transmittance by 100% and overestimated the hot spot parameter by 9%. The large leaf transmittance error is understandable upon considering the highly absorbing leaves and the consequently minor contribution of radiance scattered from lower canopy levels. In Case 11, denoting near normal solar incidence, only the LAI and leaf reflectance were retrieved with reasonable accuracy (5% and 8%, respectively) because variations in BRDF along the azimuth were lost. Generally, the BRDF becomes increasingly azimuthally symmetric as the solar zenith angle decreases, and thus, its information content also decreases (Goel and Strebel, 1983; Shultis and Myneni, 1988). In Cases 17 (planophile) and 21 (erectophile), it is evident that significant errors in retrieved parameter values occur when an incorrect LAD is used. Indeed, only the leaf reflectance and LAI (Case 17 only) were retrieved to within 10% of their correct values. Therefore, in an operational

Table 1. Red and NIR Base Case Specifications and Their Perturbations^a

| Case | Description | Solar Zenith (deg) | LAD | LAI | HSP | Leaf Refl. | Leaf Trans. | Soil Refl. |
|----------------|--------------------|-----------------------|--|-----|-----|------------|-------------|------------|
| <i>(a) Red</i> | | | | | | | | |
| 1 | Base case | 30 | Uniform | 3.0 | 4.0 | 0.0607 | 0.0429 | 0.200 |
| 3 | Dark soil | | | | | | | 0.075 |
| 5 | Low LAI | | | 1.0 | | | | |
| 7 | High LAI | | | 8.0 | | | | |
| 9 | Doubled opt. prop. | | | | | 0.1214 | 0.0858 | |
| 10 | Halved opt. prop. | | | | | 0.0304 | 0.0215 | |
| 11 | High sun | 5 | | | | | | |
| 13 | Low sun | 60 | | | | | | |
| 15 | Planophile LAD | | Planophile | | | | | |
| 17 | Planophile LAD | | Planophile (model set to uniform for inversion) | | | | | |
| 19 | Erectophile LAD | | Erectophile | | | | | |
| 21 | Erectophile LAD | | Erectophile (model set to uniform for inversion) | | | | | |
| <i>(b) NIR</i> | | | | | | | | |
| 2 | Base case | 30 | Uniform | 3.0 | 4.0 | 0.4357 | 0.5089 | 0.350 |
| 4 | Dark soil | | | | | | | 0.150 |
| 6 | Low LAI | | | 1.0 | | | | |
| 8 | High LAI | | | 8.0 | | | | |
| 12 | High sun | 5 | | | | | | |
| 14 | Low sun | 60 | | | | | | |
| 16 | Planophile LAD | | Planophile | | | | | |
| 18 | Planophile LAD | | Planophile (model set to uniform for inversion) | | | | | |
| 20 | Erectophile LAD | | Erectophile | | | | | |
| 22 | Erectophile LAD | | Erectophile (model set to uniform for inversion) | | | | | |

^a Base case values were used where data is absent.

inversion scheme, some prior knowledge of the actual LAD is highly desirable if the LAD is not made variable.

Figures 3b–d show the retrieved and correct spectral albedo, FAPAR and CPE. While spectral albedo estimates were highly accurate (below 0.5% relative error), small errors were incurred in FAPAR (up to 10%) and CPE retrievals (up to 11%). Of particular importance are Cases 7, 10, 11, 17, and 21, which yielded the poorest estimates of canopy variables. It is evident that despite significant errors in the canopy parameters, the surface state variables were well estimated in these cases.

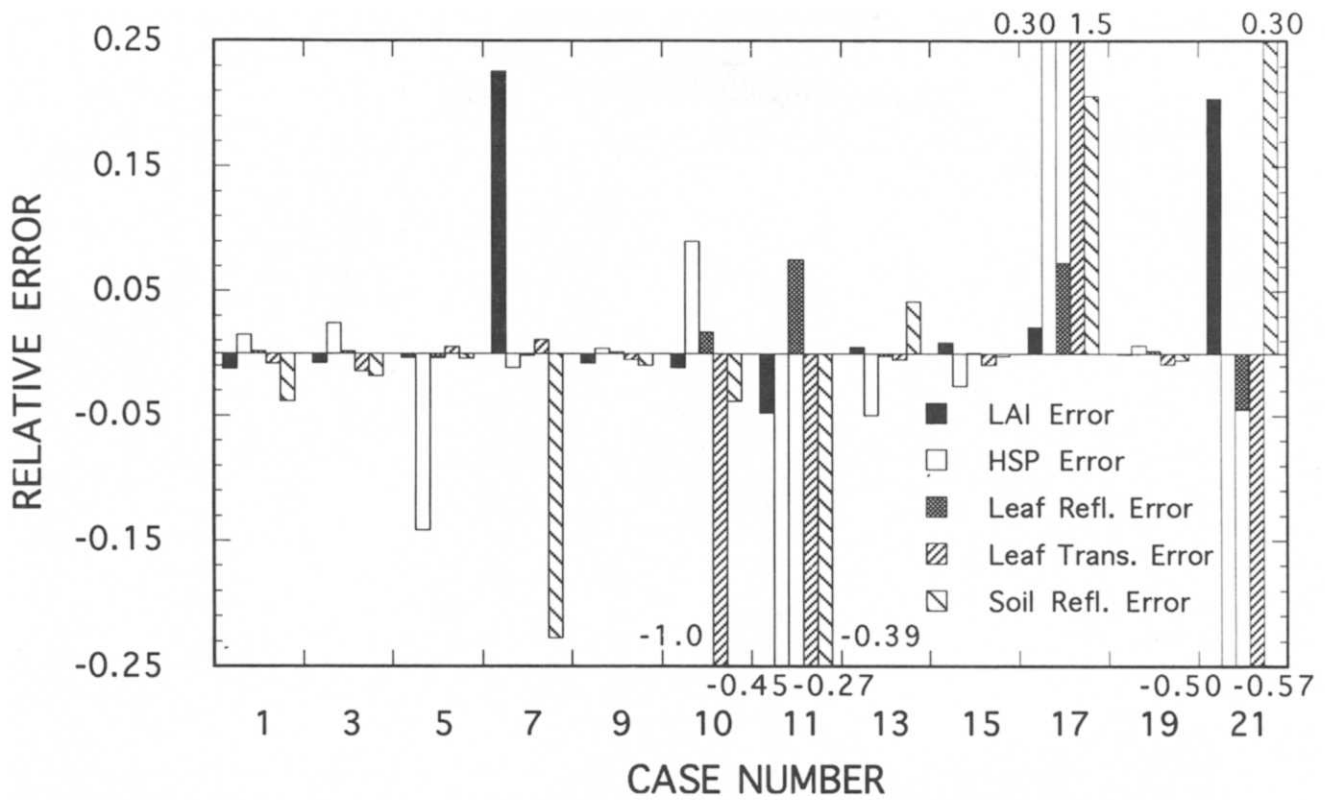
Figure 4a shows relative errors in retrieved parameters at the NIR wavelength. There is a systematic overestimation of soil reflectance (16–67% relative error) in all instances since scattering by leaves dominates the surface signal. The difficulty in accurately retrieving NIR soil reflectance is well documented (Goel and Thompson, 1984a,c). The remaining four parameters were generally retrieved to within 5% of their true

values. As might be expected, cases which were problematic in the red were similarly problematic in the NIR. Specifically, a near normal solar incidence and the use of an incorrect LAD produced the largest errors. Interestingly, while a near normal solar incidence yielded an LAI overestimation of 23% in the red, an underestimation of 27% occurred in the NIR.

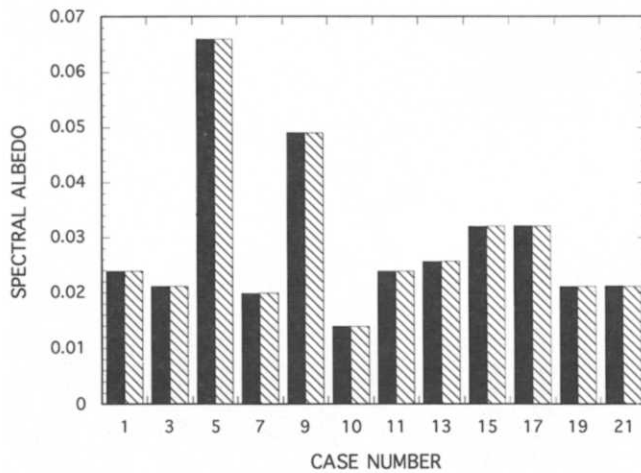
Figures 4b and 4c show differences in the NIR spectral albedo and FANIR. The retrieved spectral albedo values were highly accurate (below 1% relative error) in all cases while FANIR estimates were generally reasonable. The worst case, in which a planophile LAD was assumed, produced a 38% relative error.

SAMPLING GEOMETRIES

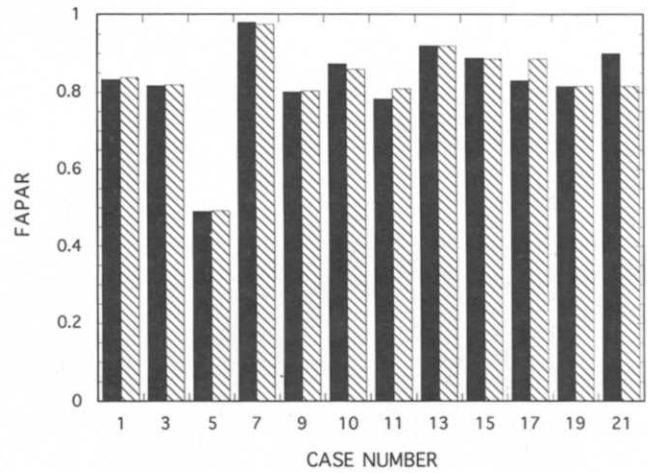
At the present time, sampling surface reflectance at 15° zenith and 45° azimuth angle increments is not feasible by satellite borne instruments. Therefore, it is of interest to assess the inversion potential using sampling geome-



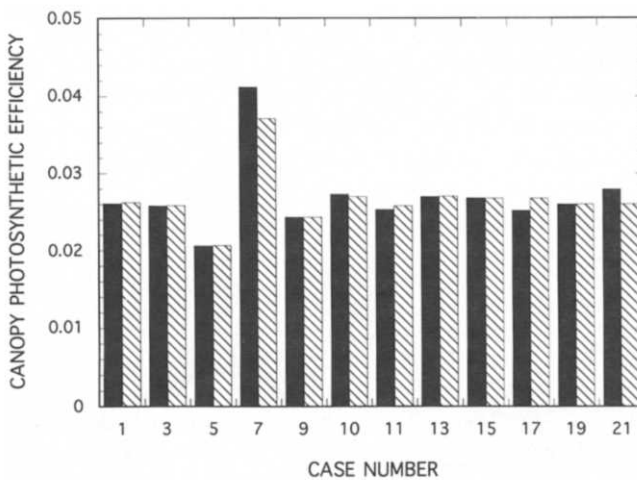
(a)



(b)



(c)



(d)

Figure 3a. Relative errors in retrieved parameters for perturbation cases at red wavelengths.

Figure 3b. Retrieved and actual spectral albedo values for perturbation cases at red wavelengths. Black bars represent retrieved values; cross-hatched bars represent actual values.

Figure 3c. Retrieved and actual FAPAR values for perturbation cases at red wavelengths. Black bars represent retrieved values; cross-hatched bars represent actual values.

Figure 3d. Retrieved and actual canopy photosynthetic efficiency (CPE) values for perturbation cases. Black bars represent retrieved values; cross-hatched bars represent actual values.

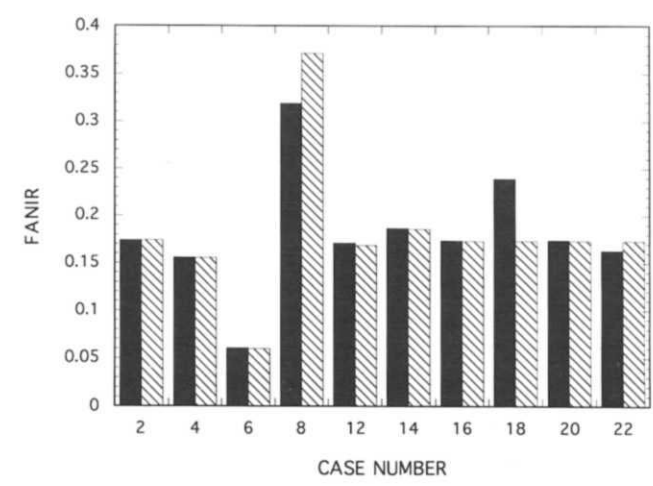
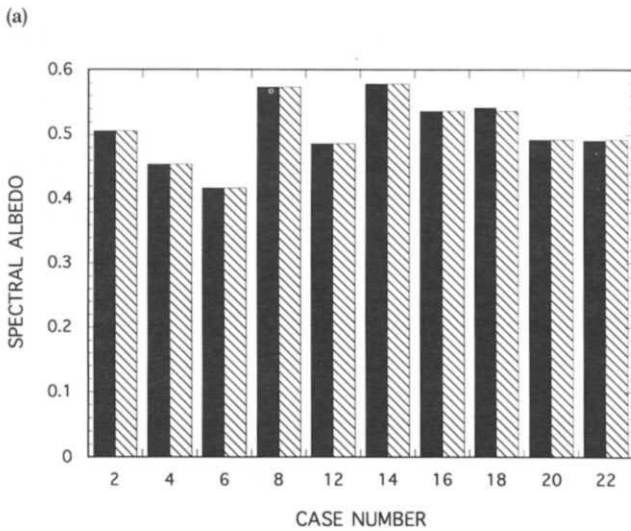
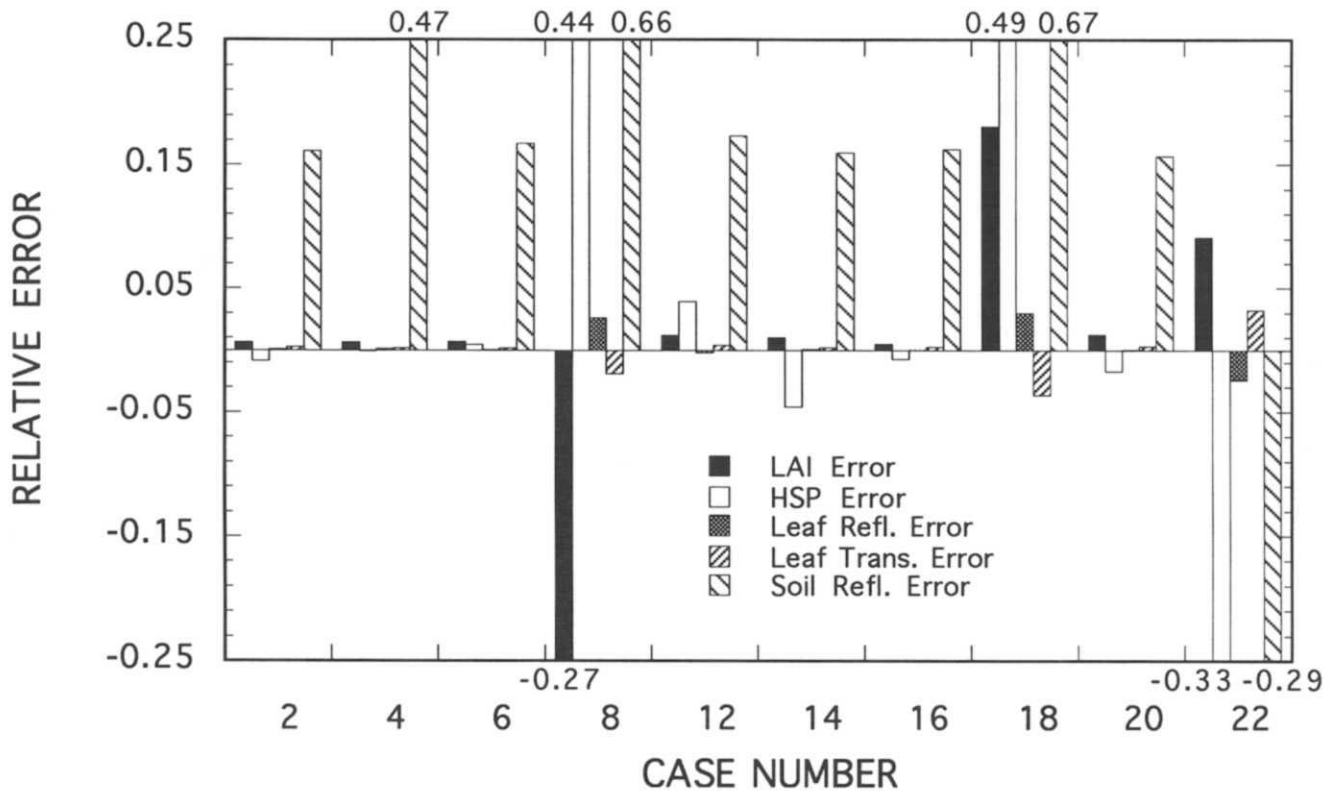


Figure 4a. Relative errors in retrieved parameters for perturbation cases at NIR wavelengths.

Figure 4b. Retrieved and actual NIR spectral albedo values for perturbation cases. Black bars represent retrieved values; cross-hatched bars represent actual values.

Figure 4c. Retrieved and actual FANIR values for perturbation cases. Black bars represent retrieved values; cross-hatched bars represent actual values.

tries of various existing and planned satellite systems. Three geometries were investigated here: the planned Multi-angle Imaging SpectroRadiometer (MISR) (Diner et al., 1989) sampling geometry in the principal azi-

muthal plane (nine view zenith angles), the MISR geometry perpendicular to the principal plane, and the NOAA-11 Advanced Very High Resolution Radiometer (AVHRR) afternoon sampling geometries realized for a

9-day period and a land target at 40° latitude. For this study, only the red and NIR base cases were investigated.

While the AVHRR scanner is advantageous due to its large view angles, daily sampling, and current operational mode, the necessity of using samples collected over multiple days is not ideal. Indeed, the temporal invariance of a true surface BRDF is by no means certain or expected. Moreover, the minimum ground instantaneous field of view (GIFOV) of 1.1 km inevitably results in some subpixel heterogeneity which cannot be accounted for in this model. While the AVHRR samples would actually be collected at unique solar angles each day, a single solar zenith angle (30°) was used in this study. The use of multiple solar zenith angles has been shown to improve minimization convergence (Goel et al., 1984); however, heliotropism may adversely affect results in some cases (Kimes and Kirshner, 1983).

Figures 5a–d show relative errors in the retrieved parameters for the various sampling geometries at red. Although both geometries retrieved all parameters to within 5% accuracy, the MISR scanning geometry in the principal plane produced errors smaller than those obtained using samples over the full hemisphere. This may be attributed to the fact that the canopy reflectance signal is most characteristic in the principal plane (Kusk, 1991a). Thus, additional samples off the principal plane appear to have a negative effect by decreasing the per-sample information content. In light of this, it is not surprising that the MISR scan geometry perpendicular to the principal plane produced the largest errors (up to 50% relative). Finally, the AVHRR geometry produced reasonably small errors (less than 8% relative). This particular geometry samples mostly in and near the principal plane.

Figures 5b–d show differences between the true and retrieved spectral albedo, FAPAR and CPE values. These variables appear to be more stable than the canopy parameters as evidenced by their relatively small errors (less than 5%). Excluding the MISR geometry perpendicular to the principal plane, all relative errors were below 1%.

Figure 6a shows relative deviations in the canopy parameters at NIR for the various sampling geometries. As in the perturbation cases, there is a systematic overestimation of soil reflectance (up to 17%). Again, sampling perpendicular to the principal plane resulted in the largest errors. However, excluding soil reflectance, all errors are well below 10% for all geometries. Excluding the MISR geometry perpendicular to the principal plane, these errors were below 2%. Figures 6b and 6c show that the NIR spectral albedo and absorbed radiation were retrieved with high accuracy (less than 1% relative error) for all sampling geometries.

ADDITION OF NOISE

A further simulation of realistic conditions was attempted by adding random gaussian noise to the synthetic BRDF values. Noise levels of 2–10% variance, at 2% increments, were tested. The mean value of the noise was zero. At each noise level, 30 realizations were inverted at both the red and NIR. The mean relative errors and standard deviations are shown in Tables 2a and 2b.

In the red wavelength, all parameters except leaf transmittance were overestimated. The hot spot parameter and soil reflectance (both means exhibiting up to about 20% relative error) were the most adversely affected by the noise. As the model was found to be least sensitive to these parameters in the sensitivity study, this result was expected. Leaf reflectance, leaf transmittance, and LAI relative errors remained below 7% for all noise levels. These were, respectively, the parameters to which the model was most sensitive in the sensitivity study. Leaf reflectance, with a maximum error of less than 2%, was retrieved most accurately. In general, most parameters exhibited an increasing error with noise. The one standard deviation confidence intervals express the sensitivity of the retrieved values to different realizations of noise. Only the leaf transmittance confidence intervals increased steadily (greater uncertainty) with greater noise. The trends in the other parameters' confidence intervals were not obvious. Leaf reflectance (< 9%) and the hot spot parameter (< 85%) represent the smallest and largest confidence intervals, respectively. Although the model was not found to be highly sensitive to the hot spot parameter in the sensitivity study, the correlated data suggest that the hot spot parameter and leaf reflectance errors may be coupled. This is plausible since strong backscatter in the red may be due to either high leaf reflectance (an optical property) or a large hot spot parameter (a structural property), or both. Therefore, these parameters may not be independent for inversion purposes.

The mean retrieved FAPAR values were slightly overestimated. All mean errors were less than 3% (less than 1% if the 2% noise value is neglected). The relative invariance of the surface state parameters, despite large errors in some canopy parameters, is consistent with the parameter perturbation and sampling geometry results. The red spectral albedo was consistently underestimated; however, all mean errors were less than 0.5%. The confidence intervals bounded errors between $\pm 2.5\%$.

As with the red inversions, most NIR parameter estimates exceeded the true parameter values — only leaf transmittance and soil reflectance were underestimated. The mean LAI, leaf reflectance, and transmittance rela-

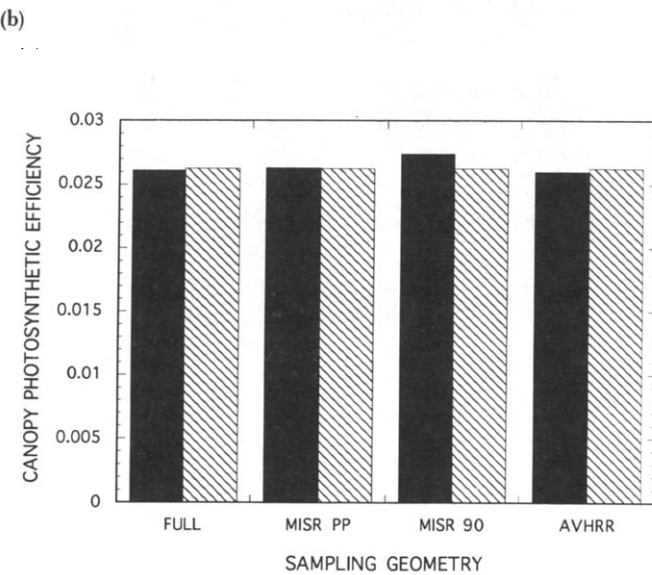
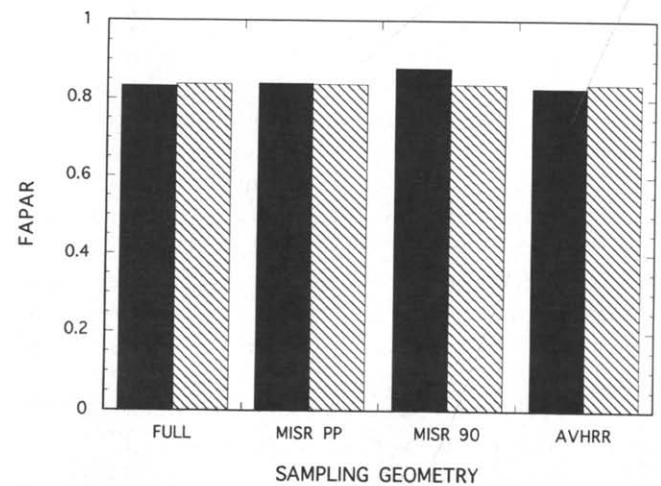
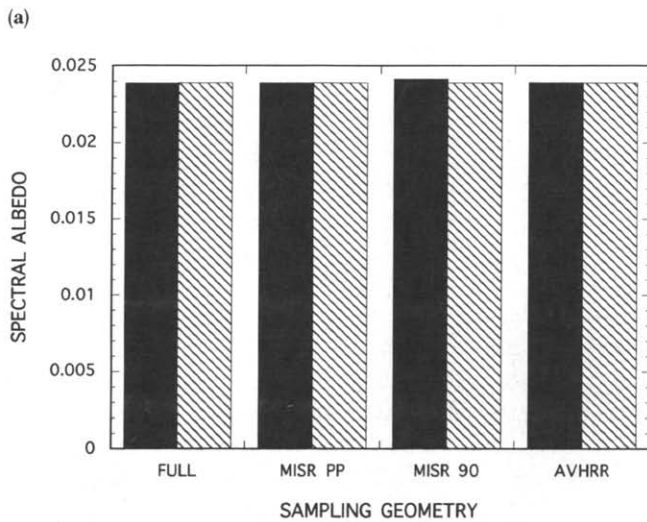
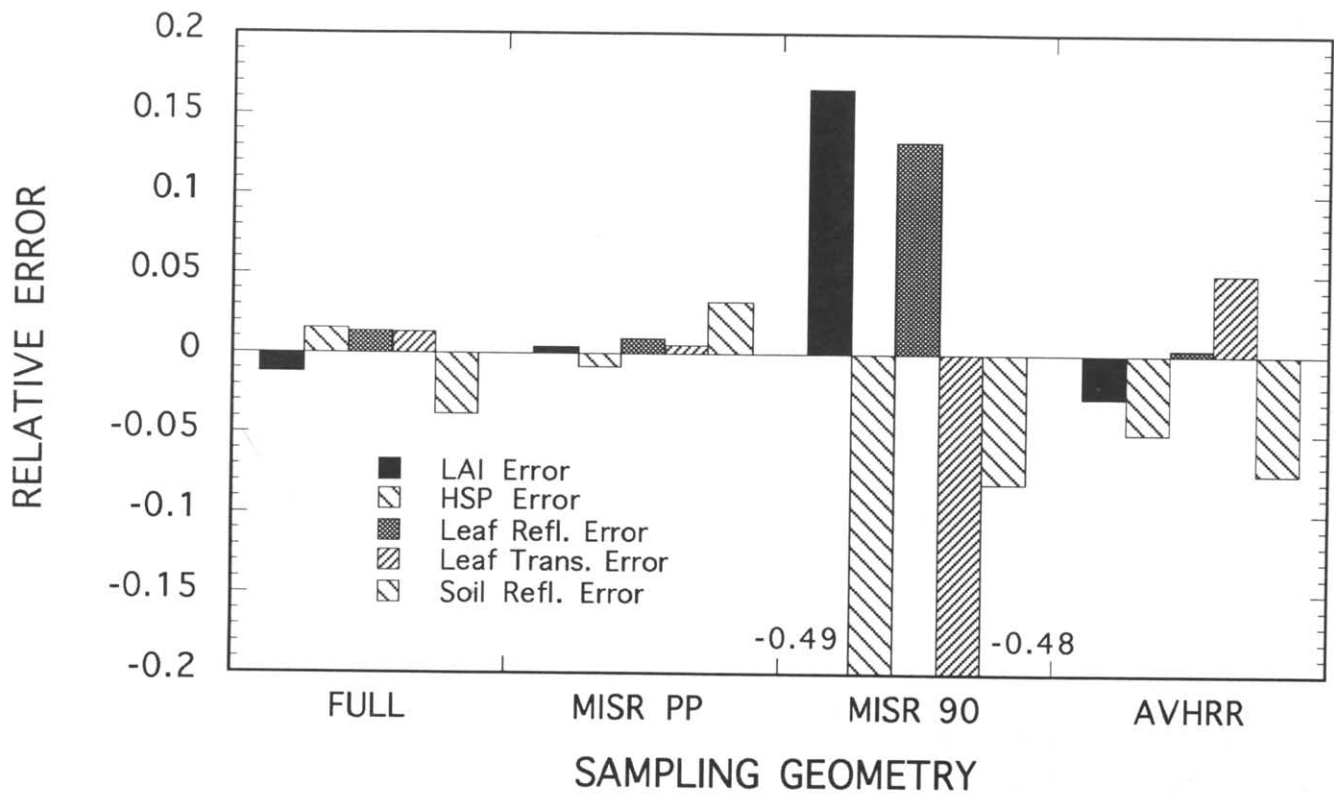
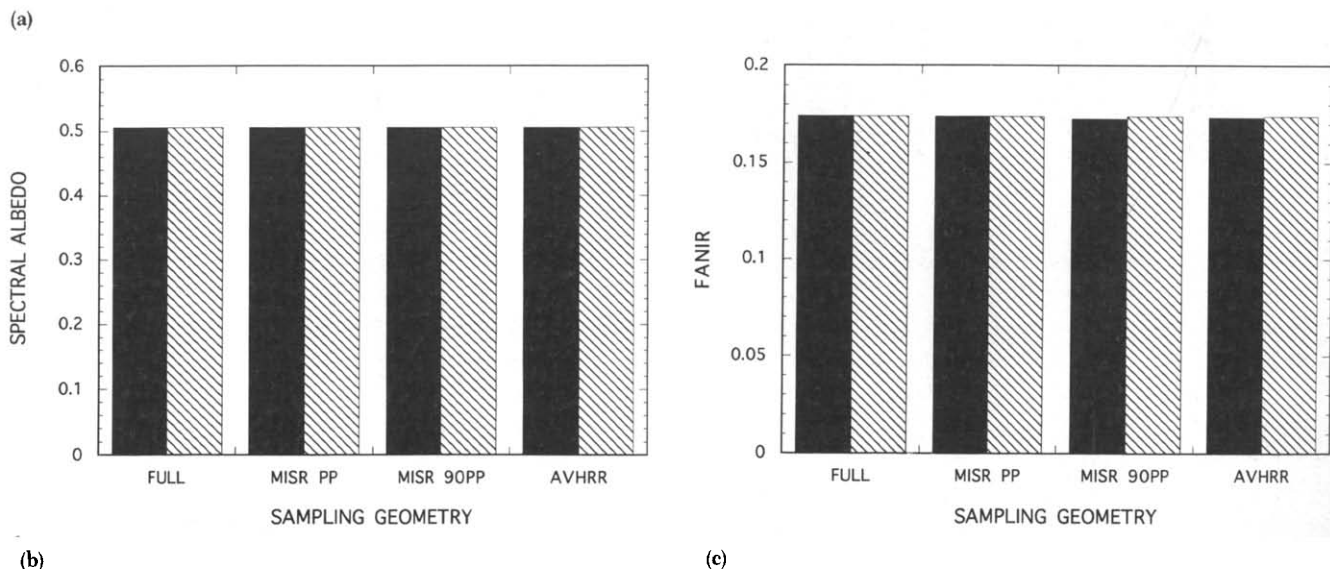
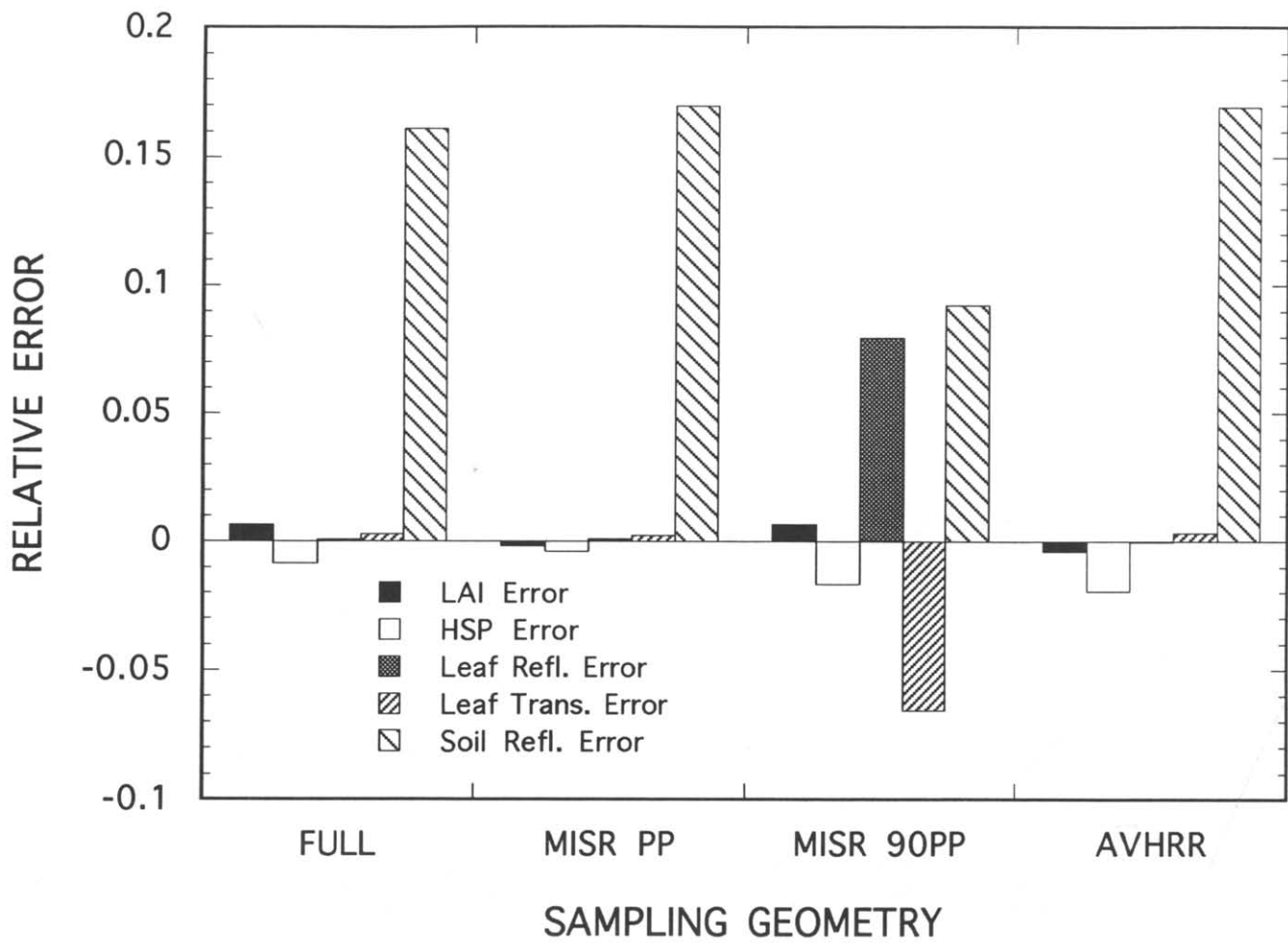


Figure 5a. Relative errors in base case inversions at red wavelengths using sampling geometries representing equal angular increments of 15° zenith and 45° azimuth (FULL), MISR view zenith angles in the principal plane (MISR PP), MISR view zenith angles perpendicular to the principal plane (MISR 90), and 9 days of NOAA-11 AVHRR afternoon passes (AVHRR).

Figure 5b. Retrieved and actual spectral albedo values for different sampling geometries at red wavelengths. Black bars represent retrieved values; cross-hatched bars represent actual values.

Figure 5c. Retrieved and actual FAPAR values for different sampling geometries. Black bars represent retrieved values; cross-hatched bars represent actual values.

Figure 5d. Retrieved and actual canopy photosynthetic efficiency (CPE) values for different sampling geometries. Black bars represent retrieved values; cross-hatched bars represent actual values.



(a) Figure 6a. Relative errors in base case inversions for different sampling geometries at NIR wavelengths (see caption for Fig. 5a).

(b) Figure 6b. Retrieved and actual NIR spectral albedo values for different sampling geometries. Black bars represent retrieved values; cross-hatched bars represent actual values.

(c) Figure 6c. Retrieved and actual FANIR values for different sampling geometries. Black bars represent retrieved values; cross-hatched bars represent actual values.

Table 2a. Mean Relative Errors and Standard Deviations of Retrieved Independent and Surface State Parameters at Red Wavelengths^a

| % Noise | LAI | | HSP | | Leaf Refl. | | Leaf Trans. | | Soil Refl. | | FAPAR | | Spectral Alb. | |
|---------|------------|----------|------------|----------|------------|----------|-------------|----------|------------|----------|------------|----------|---------------|----------|
| | ϵ | σ | ϵ | σ | ϵ | σ | ϵ | σ | ϵ | σ | ϵ | σ | ϵ | σ |
| 0.0 | -0.012 | 0.000 | 0.015 | 0.000 | 0.002 | 0.000 | -0.008 | 0.000 | -0.038 | 0.000 | -0.005 | 0.000 | -0.001 | 0.000 |
| 2.0 | 0.063 | 0.105 | 0.079 | 0.398 | 0.007 | 0.032 | 0.003 | 0.054 | 0.195 | 0.294 | 0.020 | 0.037 | -0.001 | 0.007 |
| 4.0 | 0.053 | 0.216 | 0.136 | 0.468 | 0.011 | 0.050 | -0.039 | 0.164 | 0.098 | 0.351 | 0.008 | 0.058 | -0.003 | 0.009 |
| 6.0 | 0.041 | 0.171 | 0.233 | 0.585 | 0.018 | 0.063 | -0.067 | 0.203 | 0.120 | 0.387 | 0.007 | 0.067 | -0.002 | 0.014 |
| 8.0 | 0.069 | 0.302 | 0.035 | 0.433 | 0.012 | 0.052 | -0.061 | 0.224 | 0.140 | 0.430 | 0.005 | 0.086 | -0.004 | 0.017 |
| 10.0 | 0.049 | 0.204 | 0.122 | 0.548 | 0.013 | 0.057 | -0.072 | 0.249 | 0.159 | 0.413 | 0.006 | 0.089 | -0.004 | 0.021 |

^a The base case data were inverted for 30 realizations of gaussian noise.

Table 2b. Mean Relative Errors and Standard Deviations of Retrieved Independent and Surface State Parameters at NIR Wavelengths^a

| Noise (%) | LAI | | HSP | | Leaf Refl. | | Leaf Trans. | | Soil Refl. | | FANIR | | Spectral Alb. | |
|-----------|------------|----------|------------|----------|------------|----------|-------------|----------|------------|----------|------------|----------|---------------|----------|
| | ϵ | σ | ϵ | σ | ϵ | σ | ϵ | σ | ϵ | σ | ϵ | σ | ϵ | σ |
| 0.0 | 0.006 | 0.000 | -0.009 | 0.000 | 0.001 | 0.000 | 0.003 | 0.000 | 0.161 | 0.000 | -0.001 | 0.000 | 0.000 | 0.000 |
| 2.0 | 0.001 | 0.210 | 0.153 | 0.469 | 0.013 | 0.052 | -0.008 | 0.041 | -0.039 | 0.178 | -0.027 | 0.233 | -0.001 | 0.004 |
| 4.0 | 0.031 | 0.390 | 0.227 | 0.603 | 0.028 | 0.098 | -0.016 | 0.074 | -0.112 | 0.310 | -0.041 | 0.452 | -0.002 | 0.009 |
| 6.0 | 0.028 | 0.493 | 0.333 | 0.643 | 0.049 | 0.126 | -0.029 | 0.093 | -0.128 | 0.362 | -0.069 | 0.594 | -0.003 | 0.012 |
| 8.0 | 0.073 | 0.590 | 0.295 | 0.647 | 0.055 | 0.151 | -0.032 | 0.112 | -0.110 | 0.386 | -0.026 | 0.763 | -0.005 | 0.017 |
| 10.0 | 0.033 | 0.673 | 0.427 | 0.648 | 0.098 | 0.164 | -0.057 | 0.127 | -0.178 | 0.386 | -0.146 | 0.800 | -0.006 | 0.020 |

^a The base case data were inverted for 30 realizations of gaussian noise.

tive errors were confined to less than 10%. Mean soil reflectance and hot spot parameter relative errors were as great as 18% and 43%, respectively. As with the red inversions, the NIR results were somewhat predictable based on sensitivity study results. For instance, the leaf transmittance and reflectance errors were comparable in the NIR, but the reflectance errors were substantially lower than the transmittance errors in the red. This was suggested by the model's significantly greater sensitivity to leaf reflectance in red but not in the NIR. The general increase in error with increasing noise was more perceptible in the NIR than in the red inversions. The widening of the confidence intervals with noise was evident for all parameters. Indeed, only the confidence interval limits for the leaf optical properties were reasonable (<26%). All other parameters had limits exceeding 50%. The maximum variance occurred for LAI and the hot spot parameter. This, too, follows from the sensitivity study which suggested the model was least sensitive to these parameters.

Upon comparison of the spectrally independent parameters, it appears that red reflectance data may be best suited for LAI retrieval. Indeed, although the mean errors are comparable between the different wavelengths, the standard deviations are significantly greater in the NIR. Goel and Strebel (1983) noted the higher probability of accurately retrieving LAI in the red (versus NIR) for thin canopies. It should be kept in mind that a relatively bright soil was used in this study, yet Goel et al. (1984) found that a darker soil is preferable

when trying to retrieve LAI in the NIR. While the hot spot parameter results are less clear, the red wavelength inversions again appear more reliable. The preferential use of red reflectance data for the retrieval of structural properties (e.g., the hot spot parameter and LAI) is corroborated by Kuusk (1991a).

As in the red, surface state parameter errors in the NIR were small. Both the FANIR and spectral albedo values were underestimated. The mean FANIR errors were below 15% for all noise levels, and below 8% through 8% noise. The confidence intervals for this parameter were significant, however, with the maximum limit at nearly 100% relative error for 10% noise. The mean spectral albedo errors were confined to less than 1% for all noise levels. The standard deviation envelope was confined to less than 3% error. There was no obvious correlation of the NIR surface state parameter errors with any canopy parameter errors.

These results suggest that, for up to 10% gaussian noise in the reflectance data, most parameters may be retrieved to within a reasonable error (7% at red, 10% at NIR). The relative stability of the leaf optical properties agrees with results found by Goel et al. (1984). The hot spot parameter and soil reflectance appear to be most susceptible to noise in both spectral regions. The maximum mean relative errors for these parameters were below 23% in the red and 43% in the NIR. The LAI errors varied significantly more in the NIR than in the red inversions, suggesting the latter spectral region may be preferable for LAI estimation—at least for cano-

pies of LAI < 3.0. The surface state variables appear to be more stable than the canopy parameters and apparently can be retrieved with high accuracy (<3% for all parameters except FANIR).

INVERSIONS OF FIELD DATA

The above results suggest that CANTEQ can be inverted successfully with synthetic BRDF data under various canopy and sampling conditions. To better assess the model's operational potential, inversions were conducted using field-collected directional reflectance data, including soybean (Ranson et al., 1984), red clover (Kuusk, 1991a) and barley (Kuusk, 1991a) data. These data sets were chosen because of the availability of required ancillary information.

The soybean data collected on 27 August 1980 were used in this study. The data were collected with a four-band Exotech Model 100 radiometer. Data from two spectral bands, 0.6–0.7 μm (red) and 0.8–1.1 μm (NIR), were used. The canopy reflectance was sampled at seven view zenith angles (0°, 7°, 22°, 30°, 45°, and 60°) and eight view azimuth angles (equally spaced 45° intervals) at 12 times over the day. The radiometer had a 10° instantaneous field of view (IFOV). Although the BRDF model assumes a unit steradian IFOV, the soybean data set was chosen since it has become a benchmark for several model validation and inversion studies (e.g., Goel and Thompson, 1984c; Pinty et al., 1990). However, due to the relatively large IFOV and the sharp-peaked nature of canopy hot spots (Stewart, 1990), the hot spot formulation was not included in the model for these inversions. The two-parameter Beta LAD, however, was included in CANTEQ. Hence, a six-parameter model was used. The mature soybean canopy, while exhibiting some row structure, was nearly complete (99% ground cover).

The retrieved parameters were averaged over the 12 data subsets. The mean values and standard deviations are shown in Table 3. The mean retrieved LAI is high, although the measured value is within 1 standard deviation. Closer inspection reveals that the red LAI estimate is high but the NIR estimate is excellent (0.1 absolute error). Although this contradicts the noise inversion results, the tendency for red reflectance saturation with respect to LAI at relatively low LAIs was noted by Goel and Thompson (1984c). The saturation effect may explain the poor estimate. The coefficients of the Beta LAD are close to the true values and suggest a predominantly erectophile canopy. Estimates of leaf reflectance were reasonable though slightly high. Although the red reflectance value differed by just 0.016 absolute, the measured value was outside the 1 standard deviation confidence interval. The NIR value differed by 0.041 but was within the confidence interval. Leaf transmittance was overestimated by 0.006 in the red

Table 3. True and Mean Retrieved Parameter Values with Standard Deviations for Soybean Data of 27 August 1980^a

| Parameter | True μ | Retrieved | |
|---------------------|------------|-----------|----------|
| | | μ | σ |
| LAI (both channels) | 2.9 | 4.1 | 2.5 |
| LAI (red only) | | 5.4 | 2.4 |
| LAI (NIR only) | | 2.8 | 1.9 |
| Leaf refl. (NIR) | 0.454 | 0.495 | 0.067 |
| Leaf refl. (red) | 0.073 | 0.089 | 0.006 |
| Leaf trans. (NIR) | 0.518 | 0.376 | 0.055 |
| Leaf trans. (red) | 0.064 | 0.070 | 0.028 |
| Soil refl. (NIR) | 0.232 | 0.418 | 0.127 |
| Soil refl. (red) | 0.143 | 0.133 | 0.045 |
| μ (Beta LAD) | 1.61 | 1.54 | 0.502 |
| ν (Beta LAD) | 2.18 | 2.52 | 1.03 |

^a Unless otherwise noted, retrieved values were averaged over all 12 data sets and both channels. True LAD parameter values are from Goel and Strebel (1983).

and underestimated by 0.142 in the NIR. These marginal results are somewhat confusing in light of Figure 2b, which suggests that, at LAI = 2.9, the BRDF is most sensitive to leaf reflectance and transmittance values. The red soil reflectance estimate was excellent (5% relative error). This was unexpected given the poor LAI estimate, the sensitivity analysis results, and the noise inversion results. The NIR estimate was high (80% relative error), which is consistent with the other investigations reported in this paper. The large standard deviation (30% of the mean value) follows from the noise inversion results.

There are several sources of errors that may have affected these results and deserve brief mention. Pinty et al. (1990) report evidence of a hot spot in the data. Since the hot spot formulation was not included in the model, an artificially high leaf reflectance would be retrieved. There is some azimuthal asymmetry in the data, including row structure and possibly heliotropism (Pinty et al., 1990; Camillo, 1987), which cannot be accounted for in CANTEQ. The model is further limited by assuming isotropic diffuse irradiance, a Lambertian soil reflectance and spatially homogeneous leaf distribution (no leaf clumping). Other sources of errors present in any field-gathered reflectance data include instrument and systematic experimental errors.

The 7 July 1989 red clover data (99% ground cover), 8 June 1988 and 29 June 1988 barley data (67% and 65% ground cover, respectively) from Kuusk (1991a) were also used in the inversions. This reflectance data was measured at 1° increments over the principal plane by a field goniometer / radiometer. The radiometer had bands in the red (centered at 0.675 μm) and NIR (centered at 0.810 μm) and a 1° IFOV. The small IFOV was particularly useful since the hot spot could be adequately sampled. Although this feature is essentially absent in the NIR barley data, a well-defined hot spot

is evident in the red data. Therefore, the hot spot formulation was included in the model for these inversions. This resulted in a seven-parameter model. Due to data transcription difficulties, only a subset of the recorded data was available for the inversions. Moreover, the clover data in the red was primarily from the backscatter region.

Tables 4a, 4b, and 5 show the inversion results for barley and clover data, respectively. Note that the spectrally-independent parameters (LAI, μ , and ν) were averaged over the red and NIR bands. The mean barley LAI was overestimated by 1.03 (20% relative error) for the 8 June data and by 1.53 (31% relative error) for the 29 June data. Closer inspection, however, reveals that estimates in the red were at or near the imposed parameter boundaries. Again, poor LAI estimates in the red could be the result of the reflectance saturation with LAI. The NIR values, in contrast, were underestimated. The tendency for a higher LAI estimate in the red than in the NIR differs from the noise inversion results and those of Kuusk (1991b). At NIR, the maximum leaf reflectance error was 0.027 (5.9%), and leaf transmittance error was 0.033 (6.8%). At red, relative errors in leaf optical properties varied from 32% to 204%. Kuusk (1991b) retrieved optical properties of comparable accuracy. The retrieved LAD coefficients were not consistent over the bands or data sets. At

Table 4. True and Retrieved Parameter Values for Barley Data of 8 and 29 June 1988^a

| Parameter | True | | Retrieved |
|-------------------|--------------|--|------------------------|
| | 8 June 1988 | | |
| LAI | 5.02 | | 6.05 |
| LAI (NIR) | | | 2.09 |
| LAI (red) | | | 10.0 |
| Leaf refl. (NIR) | 0.46 | | 0.488 |
| Leaf refl. (red) | 0.105 | | 0.139 |
| Leaf trans. (NIR) | 0.48 | | 0.513 |
| Leaf trans. (red) | 0.040 | | 0.121 |
| Soil refl. (NIR) | 0.225 | | 0.171 |
| Soil refl. (red) | 0.173 | | 0.209 |
| LAD (approx.) | Plagiophile | | Erectophile |
| | 29 June 1988 | | |
| LAI | 4.96 | | 6.49 |
| LAI (NIR) | | | 2.98 |
| LAI (red) | | | 10.0 |
| Leaf refl. (NIR) | 0.51 | | 0.517 |
| Leaf refl. (red) | 0.120 | | 0.169 |
| Leaf trans. (NIR) | 0.49 | | 0.483 |
| Leaf trans. (red) | 0.055 | | 0.019 |
| Soil refl. (NIR) | 0.225 | | 0.100 |
| Soil refl. (red) | 0.173 | | 0.178 |
| LAD | Erectophile | | Planophile / spherical |

^a Since the actual LAD data were not available, the description represents the idealized LAD most closely approximated by the reported foliage orientation parameters. The NIR soil reflectance was calculated based on information from Kuusk (personal communication).

Table 5. True and Retrieved Parameter Values for Clover Data of 7 July 1989^a

| Parameter | True | Retrieved |
|-------------------|------------|-------------------------|
| LAI | 4.93 | 6.64 |
| LAI (NIR) | | 3.66 |
| LAI (red) | | 9.63 |
| Leaf refl. (NIR) | 0.53 | 0.551 |
| Leaf refl. (red) | 0.11 | 0.091 |
| Leaf trans. (NIR) | 0.45 | 0.438 |
| Leaf trans. (red) | 0.03 | 0.010 |
| Soil refl. (NIR) | 0.30 | 0.303 |
| Soil refl. (red) | 0.19 | 0.300 |
| LAD | Planophile | Spherical / erectophile |

^a The LAI was measured on 5 July 1989, the optical properties were measured on 10 July 1989, and the LAD was measured on 11 July 1989. All other data were gathered on 7 July 1989. Since the actual LAD data were not available, the description represents the idealized LAD most closely approximated by the reported foliage orientation parameters. The NIR soil reflectance was calculated based on information from Kuusk (personal communication).

red, μ was greater than ν (indicating a predominantly planophile structure) for the 8 June barley data, but ν was greater than μ (indicating a predominantly erectophile structure) for the 29 June data. In the NIR, a predominantly erectophile canopy was indicated for both data sets. The true Beta parameters were not available for comparison. Soil reflectance estimates were poor in all cases except the 29 June red case (2.9% relative error). This inaccuracy was not unexpected due to the high foliage density. Finally, the hot spot parameter assumed small and relatively consistent values in both bands in the 8 June case; however, the values varied greatly (2.0 in NIR, 8.0 in red) in the 29 June case. The noticeable hot spot in the red data justifies the red estimate; however, true parameter values were not available for comparison.

The clover LAI estimates followed the barley LAI trends. The NIR estimate was slightly low (1.27 absolute error); however, the red estimate was near the imposed upper boundary. The mean LAI overestimated the true value by 35%. Again, the true optical density (LAI = 4.93) made accurate LAI estimation unlikely. The more reasonable LAI estimate in the NIR, however, allowed an accurate soil reflectance estimate (0.2% relative error). In contrast, the grossly incorrect LAI estimate in the red hampered an accurate soil reflectance estimate (58% relative error). The leaf reflectance was retrieved more accurately at NIR (4.0% relative error) than at red (17% relative error), although the absolute reflectance errors were the same (0.02). Similarly, the leaf transmittance was estimated significantly more accurately in the NIR (2.6% relative error) than in the red (88% relative error). The different LAI accuracies in the spectral bands may have dictated the accuracy of these parameters. The LAD parameters in both bands indicated a nearly spherical structure, while Kuusk (1991b) re-

ported a primarily planophile distribution. The hot spot parameter estimates were consistent (2.00) but could not be validated.

Aside from the general sources of error noted above for the soybean data, Kuusk (1991b) specifically notes a large number of phytoelements compared to number of leaves, significant noise resulting from both the canopy heterogeneity (clumping) and the small radiometer IFOV (an averaging technique was used to reduce this), and inaccuracies in the measured NIR leaf optical properties (Kuusk, 1991a). Furthermore, although the dates chosen represent those of the greatest ground cover, the barley canopies were incomplete. This spatial heterogeneity could not be replicated with the 1-D model.

Although the LAI averaged over the red and NIR channels represents a good estimate of the measured value, the tendency for the red estimate to fall on the upper boundary in the barley and clover cases makes this method somewhat subjective. Nevertheless, LAI estimates in the NIR were often accurate—particularly in the soybean cases. Leaf optical properties were well estimated for barley and clover in the NIR but not in the red. The correlation of leaf reflectance with the hot spot parameter may be responsible for some of this problem. Interestingly, the soybean leaf optical properties were slightly more accurate in the red than in the NIR. The relatively high LAI of the canopies decreases the validity of the retrieved soil reflectances. Although the LAD was accurately retrieved in some cases, the results were not consistent for the various canopies. The hot spot estimates appear reasonable but could not be validated. Finally, the barley and clover NIR results were superior to the soybean results despite the more limited sampling of the upper hemisphere. This is consistent with the results from the sampling geometry investigations. The reason for the phenomenon is not well understood but will be investigated in future work.

DISCUSSION AND CONCLUDING REMARKS

In this article, the invertibility of a highly accurate method of numerical solution of the vegetation canopy radiative transfer equation was investigated. This turbid medium 1-D model includes a hot spot approximation, leaf bi-Lambertian diffuse scattering, and specular reflection phenomena.

Several commonly used minimization routines were tested for inversion speed and accuracy. Results consistently suggested that the AMOEBA simplex method (Press et al., 1986) outperformed a Powell direction set method and a quasi-Newton method. The simplex routine, in contrast to the other methods, is generally preferred for functions with noncontinuous first and second partial derivatives or for functions that may not always be calculated accurately. The known numerical uncertainty in the reflectance calculations beyond four

decimal places may therefore have led to the performance differences among the various minimization routines.

Synthetic vegetation canopies were constructed by randomly assigning values in the physically plausible parameter domain. Through a novel principal components application, the sensitivity of the model to the five canopy parameters was evaluated for a range of LAI values. Not surprisingly, LAI and soil reflectance affected the BRDF most at low LAI values ($LAI < 1.0$), while leaf optical properties affected it most at high LAI values ($LAI > 2.0$). In both the red and NIR wavelengths, the model was nearly equally sensitive to all four parameters at an LAI of about 1.0. Furthermore, the model was significantly more sensitive to leaf reflectance than transmittance for high LAI values at red. The model was approximately equally sensitive to these two parameters at NIR. The hot spot parameter had negligible impact at all LAI values.

The model was inverted for base case synthetic canopies, plus several perturbations to the base cases, at both red and NIR wavelengths. In most cases, all parameters were retrieved to within about 5% of their true values. The worst red wavelength cases were for high LAI, near normal solar incidence angles, and low leaf optical properties. The insensitivity of the BRDF to LAI in optically thick canopies and the loss of azimuthal variations with decreasing solar zenith angle resulted in the poor retrievals. Poor leaf transmittance estimates in the case of low leaf optical properties appear linked to the low probability of multiply scattered photons exiting the canopy. In the NIR, thick canopies and near normal solar incidence angles were most problematic in terms of accurate parameter retrieval. It also appears that use of the correct leaf normal orientation is critical for accurate parameter estimation. Furthermore, surface state variables such as spectral albedos, spectral absorbed radiations (FAPAR and FANIR) and CPE were shown to be significantly less susceptible to inversion errors than are canopy parameters. Even in the worst parameter retrieval cases, these surface state variables were accurately estimated.

In an effort to simulate inversion conditions with present and planned satellite data, the effects of using MISR and AVHRR sampling geometries were investigated. It was found that sampling in the principal plane results in the most accurate parameter retrievals. Furthermore, MISR sampling perpendicular to the principal plane produced the worst retrievals. The AVHRR sampling geometry, while requiring 9 days, showed promise in retrieving canopy parameters. The surface state variables were accurately retrieved in all cases.

The effect of noise in BRDF data was also investigated by adding gaussian noise to the synthetic BRDF data. For noise with a variance of up to 10%, the impact on the retrieved parameters was minimal for

all parameters except the hot spot parameter and soil reflectance. The surface state parameters were accurately retrieved at both wavelengths. Results also suggest that LAI may be retrieved more accurately in the red than in the NIR for thin canopies ($LAI < 3.0$).

Finally, the model was inverted with soybean reflectance data sampled over the full hemisphere, and clover and barley reflectance data sampled in the principal plane. Results indicate that LAI estimates were better with NIR data. In an absolute sense, leaf optical properties were more accurate in the NIR for the barley and clover data but more accurate in the red for the soybean data. The latter is consistent with results from the sensitivity study. Soil reflectance, hot spot parameter, and LAD coefficient estimates were inconsistent.

Based on these findings, it appears that accurate numerical solutions of the radiative transfer equation, such as that by the discrete ordinates method, can be inverted and may have practical use in remote sensing applications. Several areas deserve attention, however, before an operational scheme might become practical. First, atmospheric effects that modulate the incident radiation fields were not adequately modeled in this study. The coupling of an atmospheric model to the surface BRDF is necessary to study the inversion potential of data gathered at satellite level. Second, further research is required in formulating an efficient minimization strategy. Several approaches, including redefinition of the merit function, constraints on the parameter space and different termination criteria may prove fruitful in this area. The assumption of a Lambertian soil is a poor approximation and certainly decreases the accuracy of results at low LAI values. Current plans include adding an anisotropically reflecting soil model. Presently, all sampling angles are weighted equally in merit function evaluation, yet the sampling geometry study suggests that principal plane reflectances provide the most characteristic BRDF signature. Therefore, a study in formulating the sampling weights may be useful. Finally, it is clear that some parameters may be more accurately retrieved at one wavelength than the other. By individually estimating parameters at particular wavelengths, a logical scheme might be developed which takes advantage of the information contained in the spectral signature. These topics will be the subject of our future work.

This research was performed under appointment (J. L. P.) to the Graduate Fellowships for Global Change administered by Oak Ridge Institute for Science and Education for the U.S. Department of Energy. Partial support was also provided by NASA's EOS/IDS program (R. Dickinson, PI). The support of NASA/Goddard Space Flight Center is gratefully acknowledged. In addition, we would like to thank K. J. Ranson, L. L. Biehl, and C. S. T. Daughtry for the soybean data and A. Kuusk for the clover and barley data.

REFERENCES

- Antyufeev, V. S., and Marshak, A. L. (1990), Inversion of a Monte Carlo model for estimating vegetation canopy parameters, *Remote Sens. Environ.* 33:201–209.
- Asrar, G., Myneni, R. B., Li, Y., and Kanemasu, E. T. (1989), Measuring and modeling spectral characteristics of a tall-grass prairie, *Remote Sens. Environ.* 27:143–155.
- Camillo, P. (1987), A canopy reflectance model based on an analytical solution to the multiple scattering equation, *Remote Sens. Environ.* 23:453–477.
- Chance, J. E., and LeMaster, E. W. (1977), Suits reflectance models for wheat and cotton: theoretical and experimental tests, *Appl. Opt.* 16:407–412.
- Collatz, G. J., Ball, J. T., Grivet, C., and Berry, J. A. (1991), Physiological and environmental regulation of stomatal conductance, photosynthesis and transpiration: a model that includes a laminar boundary layer, *Agric. For. Meteorol.* 54:107–136.
- Dickinson, R. E. (1983), Land surface processes and climate-surface albedos and energy balance, *Adv. Geophys.* 25: 305–353.
- Dickinson, R. E., Pinty, B., and Verstraete, M. M. (1990), Relating surface albedos in GCMs to remotely-sensed data, *Agric. For. Meteorol.* 32:109–131.
- Diner, D. J., Bruegge, C. J., Martonchik, J. V., et al. (1989), A multi-angle imaging spectroradiometer for geophysical and climatological research from EOS, *IEEE Trans. Geosci. Remote Sens.* GE-27:200–214.
- Eaton, F. D., and Dirmhirn, I. (1979), Reflected irradiance indicatrices of natural surfaces and their effect on albedo, *Appl. Opt.* 18:994–1003.
- Goel, N. S. (1988), Models of vegetation canopy reflectance and their use in estimation of biophysical parameters from reflectance data, *Remote Sens. Rev.* 4:1–213.
- Goel, N. S., and Kuusk, A. (1992), Evaluation of one dimensional analytical models for vegetation canopies, *Proc. IGARSS '92*, pp. 505–507.
- Goel, N. S., and Strebel, D. E. (1983), Inversion of vegetation canopy reflectance models for estimating agronomic variables. I. Problem definition and initial results using the Suits' model, *Remote Sens. Environ.* 13:487–507.
- Goel, N. S., and Strebel, D. E. (1984), Simple beta distribution representation of leaf orientation in vegetation canopies, *Agron. J.* 76:800–803.
- Goel, N. S., and Thompson, R. L. (1984a), Inversion of vegetation canopy reflectance models for estimating agronomic variables. III. Estimation using only canopy reflectance data as illustrated by Suits' model, *Remote Sens. Environ.* 15:223–236.
- Goel, N. S., and Thompson, R. L. (1984b), Inversion of vegetation canopy reflectance models for estimating agronomic variables. IV. Total inversion of the SAIL model, *Remote Sens. Environ.* 15:237–253.
- Goel, N. S., and Thompson, R. L. (1984c), Inversion of vegetation canopy reflectance models for estimating agronomic variables. V. Estimation of Leaf Area Index and average leaf angle using measured canopy reflectances, *Remote Sens. Environ.* 16:69–85.
- Goel, N. S., Strebel, D. E., and Thompson, R. L. (1984),

- Inversion of vegetation canopy reflectance models for estimating agronomic variables. II. Use of angle transforms and error analysis as illustrated by Suits' model, *Remote Sens. Environ.* 14:77-111.
- Kimes, D. S., and Kirchner, J. A. (1983), Diurnal variations of vegetation canopy structure, *Int. J. Remote Sens.* 4:257-271.
- Kuusk, A. (1994), A fast invertible canopy reflectance model, *Remote Sens. Environ.* (forthcoming).
- Kuusk, A. (1991a), The angular distribution of reflectance and vegetation indices in barley and clover canopies, *Remote Sens. Environ.* 37:143-151.
- Kuusk, A. (1991b), The determination of vegetation canopy parameters from optical measurements, *Remote Sens. Environ.* 37:207-218.
- Li, X., and Strahler, A. H. (1985), Geometrical-optical modeling of a conifer forest canopy, *IEEE Trans. Geosci. Remote Sens.* GE-23:705-721.
- Marshak, A. L. (1989), The effect of the hot spot on the transport equation in plant canopies, *J. Quant. Spectrosc. Radiat. Transfer* 42:615-630.
- Myneni, R. B., and Ross, J., Eds. (1991), *Photon-Vegetation Interactions*, Springer-Verlag, New York, 565 pp.
- Myneni, R. B., Gutschick, V. P., Asrar, G., and Kanemasu, E. T. (1988), Photon transport in vegetation canopies with anisotropic scattering. Parts I through IV, *Agric. For. Meteorol.* 42:1-40 and 87-120.
- Myneni, R. B., Asrar, G., Tanre, D., and Choudhury, B. J. (1992), Remote sensing of solar radiation absorbed and reflected by vegetated land surfaces, *IEEE Trans. Geosci. Remote Sens.* GE-30:302-314.
- Nilson, T., and Kuusk, A. (1989), A reflectance model for homogeneous plant canopies and its inversion, *Remote Sens. Environ.* 27:157-167.
- Norman, J. M. (1979), Modeling of complete crop canopy, in *Modification of the Aerial Environment of Plants* (B. G. Barfield and J. F. Gerber, Eds.), ASE Monograph No. 2, ASE, St. Joseph, MI, pp. 249-277.
- Norman, J. M., and Welles, J. M. (1983), Radiative transfer in an array of canopies, *Agron. J.* 75:481-488.
- Numerical Algorithms Group (1990), *The NAG Fortran Library, Mark 14, Volume 3*, NAG Inc., Downers Grove, IL.
- Pinty, B., Verstraete, M. M., and Dickinson, R. E. (1990), A physical model of the directional reflectance of vegetation canopies II. Inversion and validation, *J. Geophys. Res.* 95: 11767-11775.
- Press, W. H., Flannery, B. P., Teukolsky, S. A., and Vetterling, W. T. (1986), *Numerical Recipes*, Cambridge University Press, New York, pp. 274-312.
- Prince, S. D. (1991), A model of regional primary production for use with coarse resolution satellite data, *Int. J. Remote Sens.* 12(6):1313-1330.
- Ranson, K. J., Biehl, L. L., and Daughtry, C. S. T. (1984), Soybean canopy reflectance modeling data sets, Lab. for Appl. of Remote Sens. Tech. Report, Purdue Univ. 071584, West Lafayette, IN.
- Ross, J. K. (1981), *The Radiation Regime and Architecture of Plant Stands*, W. Junk, The Hague, The Netherlands, 391 pp.
- Shifrin, K. S. (1953), Concerning the theory of albedo, *Trans. Main. Geophys. Obs.* 101:244-257 (in Russian).
- Shultis, J. K., and Myneni, R. B. (1988), Radiative transfer in vegetation canopies with anisotropic scattering, *J. Quant. Spectrosc. Radiat. Transfer* 39:115-129.
- Stewart, R. D. (1990), Modeling radiant energy transfer in vegetation canopies, Masters Thesis, Kansas State Univ., Manhattan.
- Suits, G. H. (1972), The calculation of the directional reflectance of vegetation canopy, *Remote Sens. Environ.* 2: 175-182.
- Vanderbilt, V. C., and Grant, L. (1985), Plant canopy specular reflectance model, *IEEE Trans. Geosci. Remote Sens.* GE-23:722-730.
- Verhoef, W. (1984), Light scattering by leaf layers with application to canopy reflectance modeling: the SAIL model, *Remote Sens. Environ.* 16:125-141.
- Wessman, C. A., Ustin, S. L., Curtiss, B., and Gao, B.-C. (1991), A conceptual framework for ecosystem modeling using remotely sensed inputs, in *Proc. 5th Int. Coll. Phys. Measurements and Signatures in Remote Sens.*, ISPRS, 14-18 January 1991, European Space Agency, Paris.